TẠP CHÍ KHOA HỌC
TRƯỜNG ĐẠI HỌC QUY NHƠN

Vật liệu huỳnh quang không pha tạp phát xạ ánh sáng toàn phổ ứng dụng trong đèn LED trắng

Võ Thị Phú[1], Tạ Thị Minh Luôn[1], Đào Xuân Việt[2], Đặng Thị Tố Nữ[1], Nguyễn Minh Thông[2], Nguyễn Thị Tùng Loan[1], Lê Thị Thảo Viễn[1,*]

[1]Khoa Khoa học Tự nhiên, Trường Đại học Quy Nhơn, Việt Nam
[2]Viện đào tạo quốc tế về Khoa học Vật liệu (ITims), Trường Đại học Bách Khoa Hà Nội (HUST), Việt Nam

Ngày nhận bài: 20/06/2022; Ngày nhận đăng: 26/08/2022; Ngày xuất bản: 28/10/2022

TÓM TẮT

Vật liệu huỳnh quang không pha tạp Zn_2SnO_4 – SnO_2 kích thước cỡ vài µm đã được chế tạo thành công bằng phương pháp phản ứng pha rắn và nung ở nhiệt độ 1100 °C trong bài báo này. Vật liệu huỳnh quang này phát ánh sáng trắng tương tự như phổ ánh sáng Mặt Trời với bước sóng phát xạ trong khoảng từ 400 nm – 800 nm. Phổ phát xạ của mẫu được phân tích hàm Gauss cho các cực đại phát xạ ở các bước sóng khoảng 450 nm, 515 nm, 580 nm, 680 nm và 740 nm. Bài báo cũng giải thích nguồn gốc của các đỉnh phát xạ dựa trên lý thuyết phát xạ của các sai hỏng. Bên cạnh đó, bài báo cũng đề xuất sơ đồ giải thích nguồn gốc của các đỉnh phát xạ. Cuối cùng, khả năng ứng dụng của vật liệu trong chế tạo đèn LED chiếu ánh sáng trắng cũng được nghiên cứu trong bài báo này. Bột huỳnh quang sau khi chế tạo được phủ lên chip LED n-UV (310 nm) cho kết quả đèn LED phát ánh sáng trắng với chỉ số hoàn màu (CRI) bằng 95. Kết quả nghiên cứu cho thấy, vật liệu huỳnh quang Zn_2SnO_4 – SnO_2 có tiềm năng ứng dụng trong chế tạo LED trắng với giá thành rẻ và phương pháp đơn giản.

Từ khóa: *SnO_2 - Zn_2SnO_4, vật liệu huỳnh quang Zn_2SnO_4, vật liệu huỳnh quang toàn phổ.*

**Tác giả liên hệ chính.*
Email: lethithaovien@qnu.edu.vn

QUY NHON UNIVERSITY
JOURNAL OF SCIENCE

Full visible spectra of non-doped phosphor for WLED application

Vo Thi Phu[1], Ta Thi Minh Luon[1], Dao Xuan Viet[2], Dang Thi To Nu[1], Nguyen Minh Thong[2] and Nguyen Thi Tung Loan[1], Le Thi Thao Vien[1,*]

[1]Faculty of Natural Sciences, Quy Nhon university, Vietnam
[2]International Training Institute for Materials Science (ITIMS), Hanoi University of Science and Technology (HUST), Vietnam

Received: 20/06/2022; Accepted: 26/08/2022; Published: 28/10/2022

ABSTRACT

The Zn_2SnO_4 – SnO_2 micro-composite has been successfully fabricated by the solid reaction technique followed by calcination at 1100 °C. The obtained powder gives a full visible range from 400 nm to 800 nm. The PL spectra were fitted into five Gaussian peaks in the blue to the far-red region centered about 450 nm, 515 nm, 580 nm, 680 nm, and 740 nm. The origin of these emissions was discussed in detail. The proposed diagram for explaining the PL mechanism has been given in this paper. Further, the prepared phosphors have been coated onto the n-UV LED chip, which shows white light with a high CRI of 95. The result approves that Zn_2SnO_4 – SnO_2 micro composite is potential applications in white light-emitting diodes by a cheap and straightforward method.

Keywords: *SnO_2 - Zn_2SnO_4 powders, photoluminescence of Zn_2SnO_4, full visible spectra.*

1. INTRODUCTION

Light-emitting devices such as LEDs, WLED, and other optoelectronic devices based on wide band gap (WBG) semiconductor oxide materials are demonstrating their high efficiency and usefulness in recent years because of their regular physical, thermal and chemical properties.[1,2] One primary specification used in WLED and the lighting industry is the Color Rendering Index (CRI); thus, improving CRI for WLED is a significant and challenging task. One method commonly used to create WLED with high CRI is combining a semiconductor chip (blue or UV) with phosphors. Zinc oxide and tin dioxide are two of the most popular candidates for phosphors compared with others due to their simple synthesis and stable behavior.[3] Recently, many scientists have tried combining the two oxides ZnO and SnO_2 as a composite or compound to create new properties that suit their applications. For instance, the coupling may slow down the recombination of electron-hole pairs or improve performance in photocatalytic experiments.[4] Zn_2SnO_4-SnO_2 composite and other phases based on ZnO and SnO_2 have been produced by various methods and applied for many purposes. Abdessalem et al. synthesized the ZnO-SnO_2 nanocomposites using the sol-gel method and application on photocatalytic.[3] Precipitation – decomposition method was used to prepare the ZnO-SnO_2 composite by V.kuzhalosai et al.[5] Also, Eu^{3+} and Ca^{2+} co-doped Zn_2SnO_4 were synthesized by the hydrothermal method, and its emission was in the red band as reported by Krishna Sagar *et al.* in 2018.[6] In the same method, S. Dinesh et al. produced zinc stannate

**Corresponding authors.*
Email: lethithaovien@qnu.edu.vn

https://doi.org/10.52111/qnjs.2022.16505

(Zn_2SnO_4) and applied it in photocatalytic and antibacterial activity.[7] In addition, other shapes of Zn_2SnO_4, like nanobelts and nanorings, have been synthesized using thermal evaporation or simple chemical vapor deposition methods.[8,9] High energy milling method, electrospinning, and combustion method were also applied in the synthesis of ZnO-SnO_2 composite and Zn_2SnO_4.[10-12] Zn_2SnO_4 has a wide band gap (3.6 eV) with good potential for phosphor applications. However, only a small number of reports focus on the optical properties of these host materials.[13] Furthermore, the application of these phosphors on White LED has not been much regarded.

Normally, a phosphor consists of a host lattice and doping ions such as rare-earth ions. Specifically, Eu^{3+} and Ca^{2+} co-doped Zn_2SnO_4 was synthesized using a hydrothermal method and its emission was in the red band as reported by Krishna Sagar et al. in 2018.[12] In 2016, Dimitrievska et al. reported that Eu^{3+} doped Zn_2SnO_4, generated by a solid-state reaction method, showed several emission bands, including narrow bands of magnetic dipole emission at 595 nm and electric dipole emission at 615 nm.[13] However, phosphors based on rare-earth are not cheap and unsafe.

In this paper, the undoped phosphor SnO_2 - Zn_2SnO_4 has been successfully produced by a simple method – solid reaction. The PL spectra show a full visible range like the sunlight spectrum from 400 nm to 800 nm. When the prepared phosphor is coated onto the surface of an n-UV LED chip, the device shows warm white color with a CRI of 95. Other parameters related to the quality of WLED have been calculated. Further, the origin of PL emission and the proposed diagram for explaining the PL mechanism have been given in this research.

2. EXPERIMENTIAL

The sample synthesized by solid reaction in this work follows the below process:

i. Pure ZnO (99.99%, Sigma-Aldrich) and SnO_2 (99.99%, Sigma-Aldrich) powders were used as starting materials. The starting materials were weighed according to the stoichiometric weight ratio of 1:1 of ZnO: SnO_2 (5g ZnO and 5g SnO_2). After that, the mixture is grounded coarsely for 1 hour and further grounded by high-energy planetary ball milling (Restch PM400) at a speed of 200 rpm for 60 hours. The next step is putting the mixture into a furnace and annealing at 1100 °C.

ii. The powder was coated on to UV LED Chip.

iii. The parameters of WLED will be measured and compared with commercial products.

The prepared powders have been analyzed by X-ray diffraction (XRD) using CuKa radiation (Bruker D8 Advance) in the 2θ range of 100 – 800. The surface morphology and average size of particles are determined by ultra-high resolution scanning Electron Microscopy (SEM – Jeol JSM-7600F). In addition, the elemental analysis of the sample is studied by energy dispersive spectrometry (EDS) carried out on the Jeol JSM-7600F detector on the SEM over the range 0-20KeV. Horiba Jobin Yvon equipment was taken to investigate the luminescence characteristics at room temperature. Further, the i-DR S320A Desktop Dispensing system was used to cover the phosphor on to UV LED Chip, and the chromaticity coordinates of the phosphors were calculated by a LED testing system (Gamma Scientific).

3. RESULTS AND DISCUSSION

3.1. X-ray diffraction

Figure 1 illustrates X-ray diffraction (XRD) patterns of Zn_2SnO_4 – SnO_2 composites prepared by solid reaction and annealed at different temperatures: unanealing (a); 500 °C (b); 900 °C (c); 1000 °C (d); 1100 °C (e) and 1200 °C (f) for 2 hours in air. As shown in Figure 1, the XRD peaks of the sample annealed at 1100 °C show the highest intensity and sharpest summit. All the diffraction peaks are indexed to the cubic phase Zn_2SnO_4 (JCPDS card no. 00-024-1470, space group Fd-3m (227) and cell parameters a = b = c = 8.657 Å[14] (Figure 4a) and Tetragonal phase SnO_2 (JCPDS card no. 00-021-1250, space group

P42/mm (136) and cell constants a = b = 4.738 Å and c = 3.188 Å[15] (Figure 4b). Furthermore, as can be seen in Figure 1f, the peak (101) of the SnO_2 phase begins to separate into two peaks and form a new peak (311) of Zn_2SnO_4 at 900 °C. The same phenomenon happens at the (422) peak of Zn_2SnO_4 at 1200 °C. The formation of the second phase may cause a decrease in the photoluminescence intensity of the sample, so we chose the optimal temperature of 1100 °C in this work.

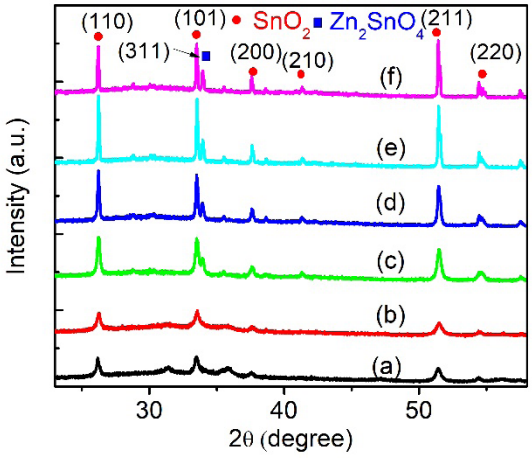

Figure 1. XRD patterns of SnO_2-Zn_2SnO_4 ample unnealed (a) and annealed at different temperature of 500 C (b); 900 °C (c); 1000 °C (d); 1100 °C (e) and 1200 °C (f).

3.2. Phosphor morphology

In order to determine phosphor morphology and size of the sample, a typical scanning electron microscope (SEM) has been carried out by ultra-high resolution scanning Electron Microscopy (SEM – Jeol JSM-7600F). Figure 2 illustrates a typical scanning electron microscope image of the prepared Zn_2SnO_4-SnO_2 at different annealing temperature un-calcinated (a); 500°C (b); 900 °C (c); 1000 °C; 1100 °C (d) and 1200 °C (f). Both particle shape and size are affected by changing calcination temperature dramatically. The powder particles of the unannealed sample (a) have an average size of about 10 nm with irregular spherical particles. When the annealing temperature increases to 1000 °C, the sample particle sizes are bigger and spherical morphology with particle bounds can be observed clearly. This result is well-matched with the XRD analysis mentioned above. The average particle size of the sample at 1100 °C is about 10 nm to 1µm, which is a suitable size for LED applications. However, under the high of temperature 1200 °C, a re-crystallization or particles cluster together to form massive or tiny particles.

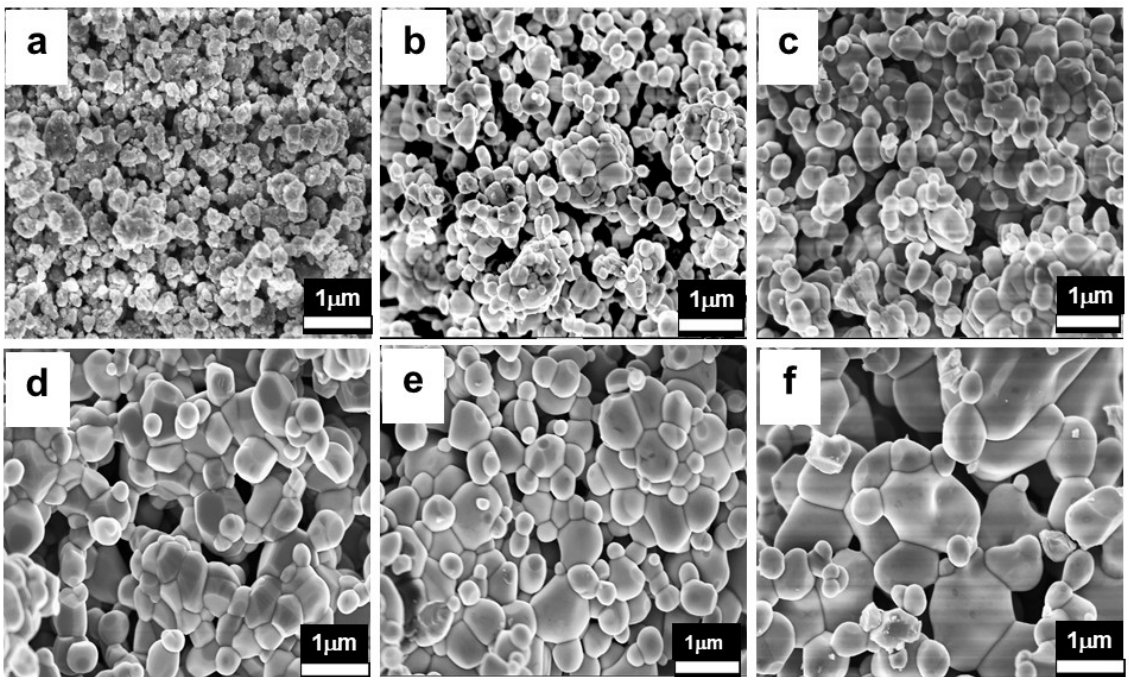

Figure 2. FESEM images of SnO_2 - Zn_2SnO_4 sample: unnealed (a) and annealed at different temperature of 500 °C (b); 900 °C (c); 1000 °C (d); 1100 °C (e) and 1200 °C (f).

https://doi.org/10.52111/qnjs.2022.16505

3.3. Optical properties

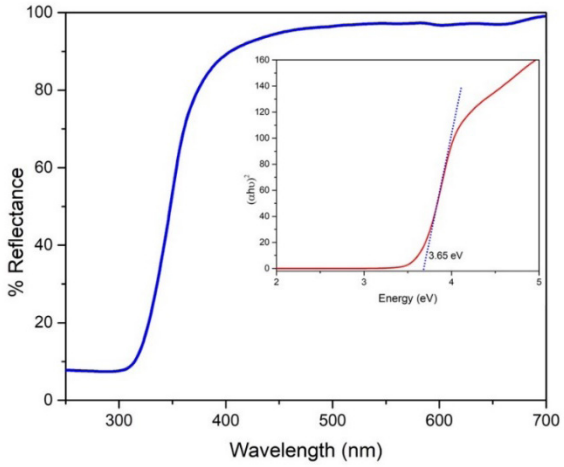

Figure 3. UV-Vis spectra of the sample Zn_2SnO_4 - SnO_2 at calcination temperature of 1100 °C.

The UV – vis spectroscopy was used to examine optical properties and estimate the band gap Eg of the prepared sample as shown in Figure 3. As seen from the Figure 3, there is a significant rise in strong light reflection around over 310 nm and the most substantial absorption at about 310 nm, which can be assigned to intrinsic band gap absorption. The K-M formula[16] has been used to estimate the optical absorption band gap of the prepared sample as shown in the inset of the Figure. The estimated value of the bandgap Eg is about 3.65 eV, which is slightly higher than the band gap value of bulk Zn_2SnO_4 (3.6 eV), but it is just under in comparison with the SnO_2 band gap (3.7 eV) reported by a previous report.[17] The two-band gaps may correspond to 3.6 eV of Zn_2SnO_4 and 3.7 eV of SnO_2 phosphor. Furthermore, based on the XRD estimated result, the two phases, Zn_2SnO_4 and SnO_2, are nearly identical.

Figure 4 illustrates the photoluminescence (PL) spectrum of the Zn_2SnO_4 – SnO_2 sample annealed with different temperature: un-calcinated (a); 500 °C (b); 900 °C (c); 1000 °C (d); 1100 °C (e) and 1200 °C (f). The spectra was recorded with the excitation wavelength 310 nm at room temperature by Nanolog - Horiba Jobin Yvon equipment. Overall, PL spectra of all samples anealed over 500 °C shows a broad visible band from 400 nm to 900 nm and nearly covers the full visible range blue – far-red emission. However, there are different intensities among them. It is observed that the PL intensity of the sample increases when the calcination temperature increases, and the highest intensity belongs to the sample with an annealing temperature of 1100 °C (the inset of Figure 4). This result is suitable with XRD and SEM results. In order to clear the origin of PL peaks emission, the broadband emission has been fitted by Gaussian function as given in Figure 4b, which indicates that the PL spectrum was fitted into five Gaussian peaks when the Gaussian was applied. Overall, there is no direct recombination process of a hole in the valence band to an electron in the conductor band because all five peaks' emission is smaller than the band gap of the prepared sample (3.65 eV). The first peak is in the blue region centered around 450 nm. Based on the calculated band gap of 3.65 eV, it is well-known from previous reports[6, 11, 18, 19] that the band gap of bulk SnO_2 and Zn_2SnO_4 are around 3.87eV and 3.6 eV, respectively. So the peak emission at 450 nm is not due to the band-to-band gap emission of neither SnO_2 nor Zn_2SnO_4 phosphor. According to a former investigation,[1, 7] the PL mechanisms have always been ascribed to other luminescent centers, such as oxygen vacancies and residual strain during the growth process. Hence, this work supports that the blue in the PL spectra can be attributed to oxygen vacancy defects in the SnO_2. The second band emission centered around 515 nm. This peak's origin was also discussed in Fu et al. research[20] and Baruah et al. report.[21] According to them, the similar broad green emission centered at 520 nm in Zn_2SnO_4 under Xenon lamp excitation was caused by oxygen vacancy in Zn_2SnO_4 during the growth process. Moreover, Smilja et al. said that the 546 nm emission in ZnO/SnO_2 spectra were that green emission implicates surface defects, as well as the defects just below the crystalline surface.[22] So we suggest that the emission centered at 515 nm observed in PL spectra relates to oxygen

vacancies in Zn_2SnO_4. Next, the third peak is in the yellow-orange region centered at 580 nm, which may attribute to SnO_2 defects such as Zn interstitials (Z_{ni}) or oxygen interstitials (O_i).[8] The two final peaks are red and far-red, centered at 680 nm and 740 nm, which have not been observed and discussed in previous reports. We suggest that they may relate to surface defects of the obtained sample,[23] but the exact type and number of defect states depend on the method and parameters changing in the process.

Regarding the origin of the red emission band, Fu et al.[20] approved that stoichiometry Zn/Sn played a role in this emission. Furthermore, the red emission centered at 630 nm in SnO_2 PL spectra reported by Smilja et al.[22] was considered related to deep–level defects within the gap of SnO_2, associated with oxygen vacancies and Sn interstitial formed during the synthesis procedure. The origin of this emission is still unclear and needs another measurement. Nevertheless, we agree with Chih-Hsien Cheng et al.[23] that the origin of the infrared 700 nm in his research is related to the transition states between neutral and ionized oxygen. In addition, from what is discussed above and what is shown in PL spectra, we propose a diagram to explain the PL mechanism as shown in Figure 5. We believe defects formed during the calcination process play as energy states within the band gap. Hole traps are states that exit just over the valance band and fill holes, whereas electron traps are formed just under the conductor band and fill with electrons. The PL mechanism can be proposed as the following explanation. First, electrons from the valance band absorb excited energy as large as band gap energy and move to the conductor band to become excited electrons. Because the electron traps are just under the conductor band, excited electrons are trapped in electron traps easily without light-emitting. After that, these electrons release to lower energy states and depend on the gap between the two states that emit blue, green, red, or infrared.[24]

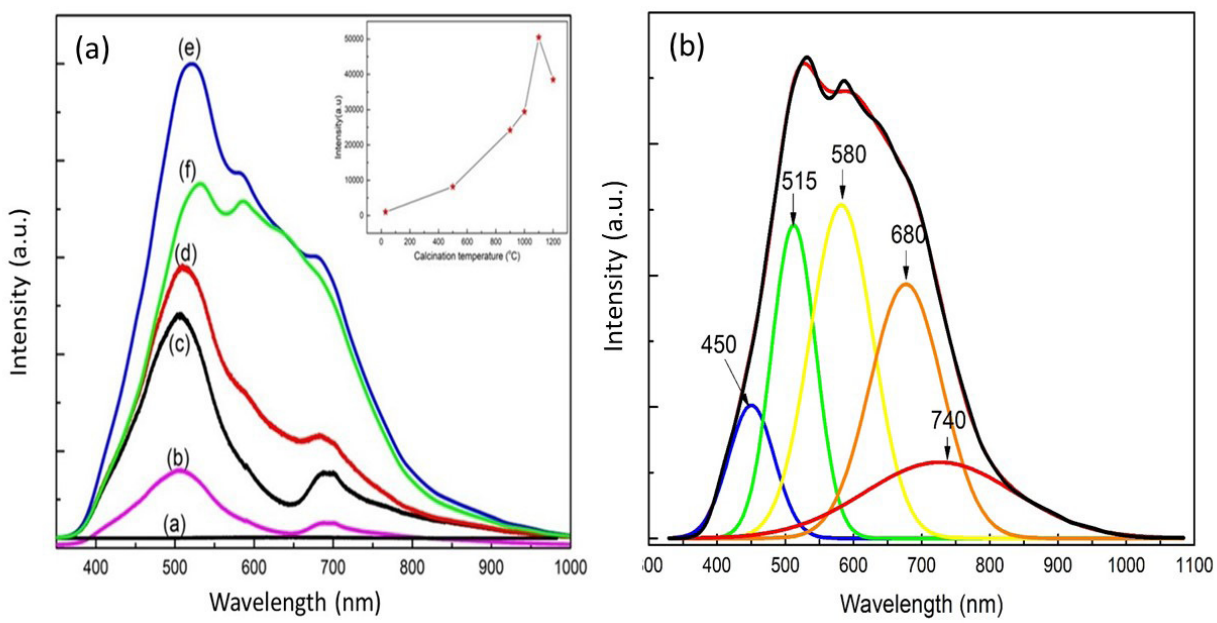

Figure 4. PL spectra of the Zn_2SnO_4 – SnO_2 phosphor annealed at different calcination temperatures (a) and PL of the sample annealed at 1100 °C fitted by Gaussian peak (b). The inset of the Figure a is the relative intensity of the Zn_2SnO_4 – SnO_2 phosphor annealed at different calcination temperatures.

https://doi.org/10.52111/qnjs.2022.16505

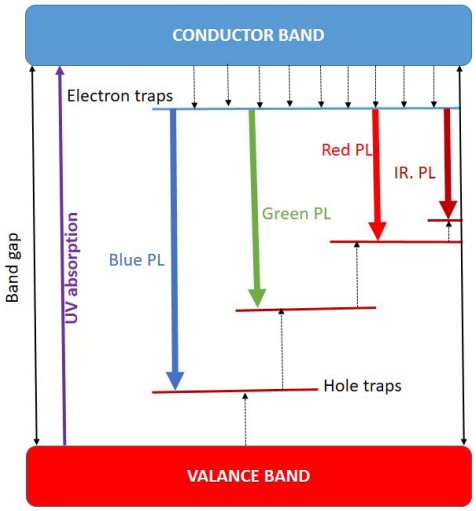

Figure 5. Proposed energy band diagram for expalination PL machanism of Zn_2SnO_4 – SnO_2 sample showing the defect states and the transitions between the states.

3.4. Electroluminescence properties of Zn_2SnO_4 – SnO_2 micro composite

In order to explore the potential application of Zn_2SnO_4 – SnO_2 powder annealed at 1100 °C, white emission LED is assembled by coating 5 mg of Zn_2SnO_4 – SnO_2 phosphor on an LED chip 310 nm by the i-DR S320A Desktop Dispensing system. The image of the white LED device underdrive current of 0.2004 A and a voltage of 8.029 V during the process, and its CIE chromaticity coordination is displayed in Figure 6. The Zn_2SnO_4 – SnO_2 powder annealed at 1100 °C was covered on. The device was then introduced into an integrating sphere system to calculate parameters related to the quality of WLED as shown in Table 1. Figure 6 demonstates that the CIE coordinates and CRI of White LED are (0.3755; 0.4173) and 95, respectively, which are very close to natural light. The colour temperature is 4273 K, which is energizing and most closely mimics natural daylight; it helps with tasks requiring focused attention, such as reading, computer work, carpentry, and drawing. These results demonstrate that Zn_2SnO_4 – SnO_2 micro composite phosphor shows a potential application in producing high both CRI and LER White LED.

Table 1. The WLED parameters (D_{uv}; Correlated colour temperature (CCT); Colour rendering index (CRI); Luminous efficacy of radiation (LER); R_9 and CIE coordinates(x,y)) of LED covered phosphor.

Sample	LED parameters						
	D_{uv}	CCT (K)	CRI	LER (lm/W)	R_9	x	y
Zn_2SnO_4 – SnO_2	0.0194	4273	95	85	94	0.3755	0.4173

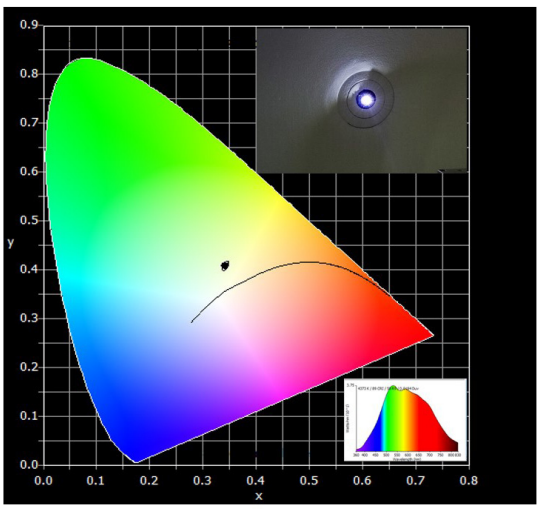

Figure 6. CIE 2015-10° xy color chromaticity coordinates of the spectral emission from UV LED chip coated by prepared phosphor. The insets is the electroluminescence spectrum and the image captured by a digital camera of the white-emitting LED.

4. CONCLUSION

The Zn_2SnO_4 – SnO_2 micro composite was produced successfully by solid-state reaction followed by calcination at 1100 °C in air. The crystalline structure of samples was mixed of the cubic phase Zn_2SnO_4 (JCPDS card no. 00-024-1470, space group Fd-3m (227) and cell parameters a = b = c= 8.657 Å) and Tetragonal phase SnO_2 (JCPDS card no. 00-021-1250, space group P42/mm (136) and cell constants a = b = 4.738 Å and c = 3.188 Å. PL spectra of all samples show a broad visible band from 400 to 900 nm, nearly covering the full visible range of blue–far–red emission with peaks at around 450, 515, 580, 680, and 740 nm. A PL mechanism diagram has been proposed to explain the emission's origin. The LED chip 310 was used to cover obtained phosphor, getting a white LED. The CIE coordinates and CRI of White LED are (0.3755:0.4173) and 95, respectively. These results demonstrate that Zn_2SnO_4 – SnO_2 micro composite phosphor is potentially applicable in producing high CRI White LED.

Acknowledgement. *This research is conducted within the framework of science and technology projects at institutional level of Quy Nhon University under the project code T2022.747.03.*

REFERENCES

1. Y. N. Ahn, K. D. Kim, G. Anoop, G. S. Kim & J. SooYoo1. Design of highly efficient phosphor converted white light-emitting diodes with color rendering indices (R_1 − R_{15}) ≥ 95 for artificial lighting, *Scientific Reports,* **2019,** *9,* 16848813.
2. J. Shi, J. Zhang, L. Yang, M. Qu, D. C. Qi. Wide bandgap oxide semiconductors: from materials physics to optoelectronic devices, *Advanced Materials*, **2021**, *33*, 2006230.
3. A. Hamrouni, N. Moussa, F. Parrino, A. D. Paola, A. Houas, and L. Palmisano. Sol-gel synthesis and photocatalytic activity of ZnO-SnO_2 nanocomposites, *Journal of Molecular Catalysis A: Chemical*, **2014**, *390,* 133–141.
4. K. A. Omar, B. I. Meena, and S. A. Muhammed. Study on the activity of ZnO-SnO_2 nanocomposite against bacteria and fungi, *Physicochemical Problems of Mineral Processing*, **2016**, *52*(2), 754–766.
5. V. Kuzhalosai, B. Subash, A. Senthilraja, P. Dhatshanamurthi, and M. Shanthi. Synthesis, characterization and photocatalytic properties of SnO_2-ZnO composite under UV-A light, *Spectrochimica Acta Part A: Molecular and Biomolecular Spectroscopy*, **2013**, *115*, 876–882.
6. K. Sagar, C. Kuttykrishnan, and J. B. Mohammed. Hydrothermal growth of Zn_2SnO_4: Eu , Ca for red emission, *Journal of Luminescence*, **2018**, *33*, 675-6804.
7. S. Dinesh, S. Barathan, V. K. Premkumar, G. Sivakumar, and N. Anandan. Hydrothermal synthesis of zinc stannate (Zn_2SnO_4) nanoparticles and its application towards photocatalytic and antibacterial activity, *Journal of Materials Science: Materials in Electronics*, **2016**, *27*(9), 9668–9675.
8. Q. R. Hu. Synthesis and photoluminescence of Zn_2SnO_4 nanowires, *Journal of Alloys and Compounds,* **2009**, *484*(1–2), 25–27.
9. Q. Li. Preparation of Zn_2SnO_4/SnO_2: Mn_2O_3 microbox composite materials with enhanced lithium-storage properties, *ChemElectroChem*, **2017**, *4*(6), 1334–1340.
10. L. Ma, S. Y. Ma, H. Kang, X. F. Shen, T. T. Wang, X. H. Jiang, Q. Chen. Preparation of Ag-doped ZnO-SnO_2 hollow nanofibers with an enhanced ethanol sensing performance by electrospinning, *Materials Letters*, **2017**, *209*, 188–192.
11. L. C. Nehru and C. Sanjeeviraja. Processing Research Controllable growth of Zn_2SnO_4 nanostructures by urea assisted microwave-assisted solution combustion process, *ChemElectroChem,* **2013**, *14*(5), 606–609.
12. L. Manzato, D. M. Trichês, S. Michielon de Souza, and M. Falcão de Oliveira. Synthesis of nanostructured SnO and SnO_2 by high-energy milling of Sn powder with stearic acid, *Journal of Materials Research*, **2013**, *29*(1), 84–89.

13. L. T. T. Vien, N. Tu, D. X. Viet, D. D. Anh, D. H. Nguyen and P. T. Huy, Mn^{2+}-doped Zn_2SnO_4 green phosphor for WLED applications, *Journal of Luminescence*, **2020**, *227*(117522), 1-9.

14. M. Asemi, M. Ghanaatshoar. Boosting the photovoltaic performance of Zn_2SnO_4-based dye-sensitized solar cells by Si doping into Zn_2SnO_4, *Journal of the Amercan ceramic society*, **2017**, *100*, 5584-5592.

15. Y. Gao, M. Hou, Z. Shao, C. Zhang, X. Qin and B. Yi. Highly effective oxygen reduction activity and durability of antimonydoped tin oxide modified PtPd/C electrocatalysts, *RSC Advances,* **2016**, *5*, 1-8.

16. J. Tauc. Optical properties and electronic structure of amorphous Ge and Si, *Materials Research Bulletin*, **1968**, *3*(1), 37–46.

17. T. Jia, J. Zhao, F. Fu, Z. Deng, W. Wang, Z. Fu, F. Meng. Synthesis, characterization, and photocatalytic activity of Zn-doped SnO_2/Zn_2SnO_4 coupled nanocomposites, *International Journal of Photoenergy*, **2014**, 1–7.

18. P. Wu. Correlation between photoluminescence and oxygen vacancies in In_2O_3, SnO_2 and ZnO metal oxide nanostructures, *Journal of Physics: Conference Series*, **2009**, *188*(1), 12054.

19. A. Gaber, M. A. Abdel- Rahim, A. Y. Abdel-Latief, and M. N. Abdel-Salam. Influence of calcination temperature on the structure and porosity of nanocrystalline SnO_2 synthesized by a conventional precipitation method, *International Journal of Electrochemical Science*, **2014**, *9*(1*)*, 81–95.

20. N. Duy, T. Luu, M. Quynh, L. V. Vu, and N. Ngoc. Phase transformation and photoluminescence of undoped and Eu^{3+} -doped zinc stannate (Zn_2SnO_4) nanocrystals synthesized by hydrothermal method, *Journal of Materials Science: Materials in Electronics*, **2018**, *110*(10), 109-120.

21. S. Yang and J. Zhang. Orange photoluminescence emission and multi-photon Raman scattering from microscale Zn_2SnO_4 tetrapods, *Chemical Physics Letters,* **2018**, *208*, 209-212.

22. S. Marković, A. Stanković, J. Dostanić, L. Veselinović, L. Mančić, S. D. Škapin, Dražič, I. Janković-Častvan, D. Uskoković. Simultaneous enhancement of natural sunlight- and artificial UV-driven photocatalytic activity of a mechanically activated ZnO/SnO_2 composite, *RSC Advances*, **2017**, *7*(68), 42725–42737.

23. C. H. Cheng, W. L. Hsu, C. J. Lin, Y. H. Pai, and G. R. Lin. Performance of highly transparent and stable zinc oxide co-doped thin-film by aluminum and ytterbium, *Journal of Display Technology,* **2014**, *10*(10), 786–792.

24. L.T.T. Vien, N. Tu, T. M. Trung, N. V. Du, D.H. Nguyen, D. X. Viet, N.V. Quang, D. Q. Trung, P. T. Huy. A new far-red emission from Zn_2SnO_4 powder synthesized by modified solid state reaction method, *Optical materials*, **2020**, *100*(109670), 1-9.